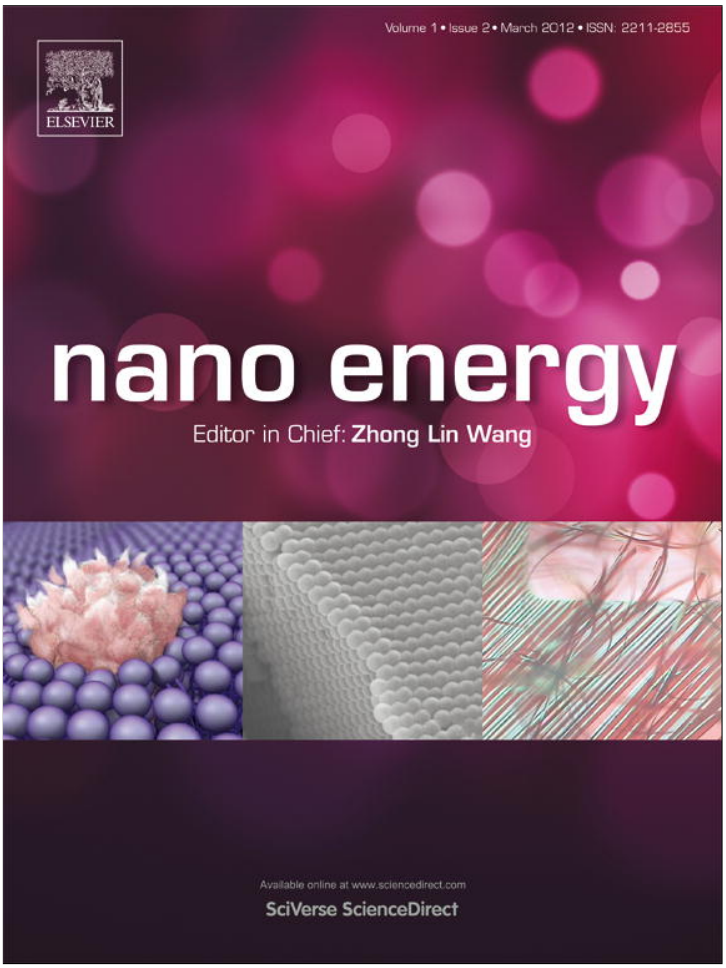

Nano Energy (2012) 1, 259–272

Available online at www.sciencedirect.com

SciVerse ScienceDirect

journal homepage: www.elsevier.com/locate/nanoenergy

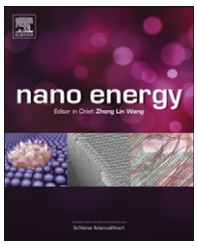

REVIEW

Hybrid cells for simultaneously harvesting multi-type energies for self-powered micro/nanosystems

Chen Xu, Caofeng Pan, Ying Liu, Z.L. Wang*

School of Materials Science and Engineering, Georgia Institute of Technology, Atlanta, GA 30332-0245, USA

Received 20 December 2011; accepted 4 January 2012
Available online 13 January 2012

KEYWORDS
Nanogenerator;
Hybrid cell;
Self-powered system;
Biofuel cell;
Solar cell

Abstract
Our living environment has an abundance of energies in the forms of light, thermal, mechanical (such as vibration, sonic wave, wind, and hydraulic), magnetic, chemical, and biological. Harvesting these types of energies is of critical importance for long-term energy needs and sustainable development of the world. Over the years, rationally designed materials and technologies have been developed for converting solar and mechanical energies into electricity. Photovoltaic relies on approaches such as inorganic *pn* junctions, organic thin films, and organic-inorganic heterojunctions. Mechanical energy generators have been designed based on principles of electromagnetic induction and piezoelectric effect. Innovative approaches have to be developed for conjunctional harvesting of multiple types of energies using an integrated structure/material so that the energy resources can be effectively and complimentarily utilized whenever and wherever one or all of them are available. We give a review on the hybrid cells that are designed for simultaneously harvesting solar and mechanical, and chemical and mechanical energies using nanotechnology. The two energy harvesting approaches can work simultaneously or individually, and they can be integrated in parallel and series for raising the output current and voltage, respectively. Innovative approaches have been demonstrated for developing integrated technologies for effectively scavenging available energies in our environment around the clock.

Introduction

Most of today's energy comes from the fossil fuel, which unfortunately produces a considerable amount of CO_2 emission that causes numerous problems. To ensure sustainable development of our society, we must not only develop renewable energy courses but also find other innovative solutions to the problem. Currently, the renewable energy comprises only 5.14% of the energy production [1] worldwide (Fig. 1), so considerable effort has gone to renewable energy harvesting [2], such as solar [3–10], hydroelectric [11,12], wind [13], and hydrothermal energy [14,15].

*Corresponding author.
E-mail addresses: zlwang@gatech.edu, zhong.wang@mse.gatech.edu (Z.L. Wang).

2211-2855/$ - see front matter © 2012 Elsevier Ltd. All rights reserved.
doi:10.1016/j.nanoen.2012.01.002

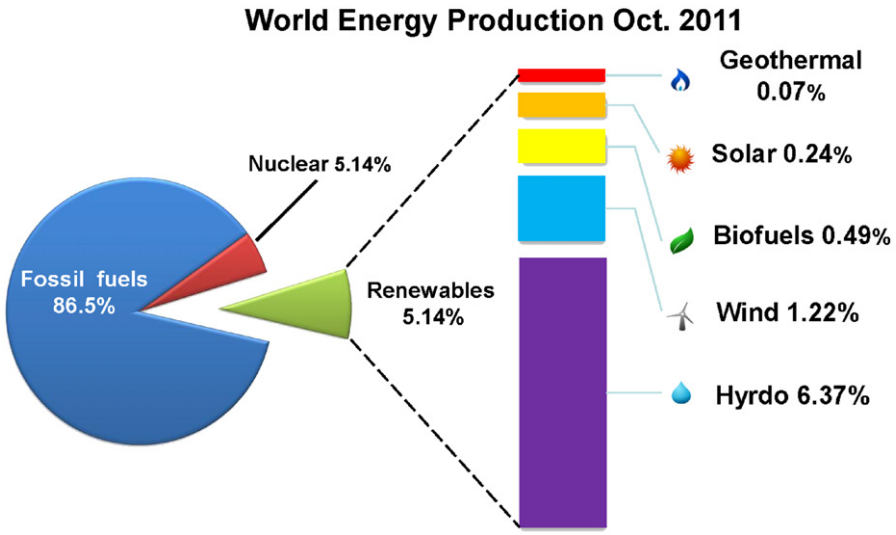

Figure 1 Pie chart of the world energy production in October 2011 with the renewable distribution.

Although it is rather challenging to solve the large-scale world energy need, energy harvesting is a technology by which ambient energy is extracted from the environment and converted into electricity to power electronic devices. Researchers have developed several approaches for harvesting solar, thermal, mechanical, and chemical energies, but all of the approaches are targeted at one type of energy for one type of particular applications, while the rest of the other types of energies are wasted. A solar cell, for example, is only designed to harvest the energy from the sun, but the energy from the heat generated by the sun light is ignored. To fully utilize the energy in the environment, a hybrid cell [16] (HC) has been first proposed by Wang's group for simultaneously harvesting multi-type energies using a single generator (e.g., a hybrid cell that harvests both solar and mechanical energy [17] instead of one single source). As the number of personal electronics and mobile electronics is rapidly increasing, we desperately need technologies that can achieve maintenance-free and sustainable operation of micro-electromechanical systems (MEMS), wireless electronics, and biomedical sensors. The hybrid cells are being developed to fully utilize the energies that are available to us.

Semiconductor one-dimensional nanostructures [18,19], a subset of these materials, have received significant attention for their unique properties and complex structures especially in energy harvesting technology. Many nanostructure-based materials are promising candidates for multi-type energy harvesting devices. The birth of HC devices could be important for developing innovative technologies towards maintenance-free, self-powered systems [20] without batteries or at least extend the lifetime of batteries. This is particularly attractive for wireless sensor networks, environmental monitoring, biomedical devices, and personal electronics.

This review summarizes the basic principles and approaches of HCs that have been developed using nanowires. Some basic applications for powering UV sensor, pressure sensor, and LED will be illustrated. We anticipate that the article will stimulate relevant research in the field so that the hybrid cell can be a distinct and disciplinary in the field of energy science and technology.

The importance of multi-type energy harvesting

In the working environment of a nanosystem or microsystem, the energy available for driving the system could vary from time to time and from location to location. This is especially true for mechanical vibration energy and solar energy. Solar is probably the most abundant energy that we are interested in, but solar is not always available, strongly depending on day, night, and weather. Mechanical energy is location-dependent, which may not be suitable for mobile electronics. To effectively utilize the energies that are available at a given time and location, a generator is required for converting all types of energies, such as solar, thermal, mechanical, and chemical, into electricity. A wireless environmental sensor, for example, is an emerging technology that can reliably measure various conditions in civil, aerospace, and biomedical applications. One of the major drawbacks of wireless sensors is that they require considerable power. In some remote locations, supplying power through cables, or using disposable energy sources, is often impractical, if not impossible.

Thus developing HCs according to a systematic approach would be highly advantageous. After the first nanowire-based HC device was demonstrated for concurrently harvesting solar and mechanical energy in 2009 [16], it inspired a number of researchers to work on developing such technology. Since then, many more HCs for multi-type energy harvesting including biomechanical and biochemical energies and also solar and acoustic energies have been demonstrated. The following sections will review several innovative ways in which multi-type energies can be harvested based on nanostructure-based HCs.

Hybrid cell: from mono- to multi-type energy harvesting

Photovoltaic cells or solar cells are a popular renewable energy technology. However, solar cells do not work well without sufficient sun light, necessitating a supplementary battery for the harvesting system and limiting their adaptability to certain applications. Considering the fact

that mechanical energy is widely available in our living environment, we first demonstrate an approach for simultaneously harvesting solar and mechanical energies.

The prototype: a hybrid cell for solar and mechanical energies

In 2009, Xu et al. developed a hybrid cell [16] (HC) for harvesting solar and mechanical energies. It is a simple integration of a dye-sensitized solar cell [5,21,22] (DSSC) and a piezoelectric nanogenerator [23–25] (NG) on a common substrate, as schematically shown in Fig. 2c. The HC utilized ZnO nanowires (NWs) in both the DSSC and NG units for solar energy and mechanical energy harvesting. An equivalent circuit of the serially connected hybrid cell (s-HC) composed of DSSC and NG is shown on the right-hand side of Fig. 2c.

The HC includes three main parts: ZnO NWs for DSSC (Fig. 2a), a zigzagged electrode, and the ZnO NWs for NG [23] (Fig. 2b). The cathode of the NG and the anode of the DSSC were integrated on the same silicon substrate, which formed a serially connected SC and NG. The continuous ZnO thin film

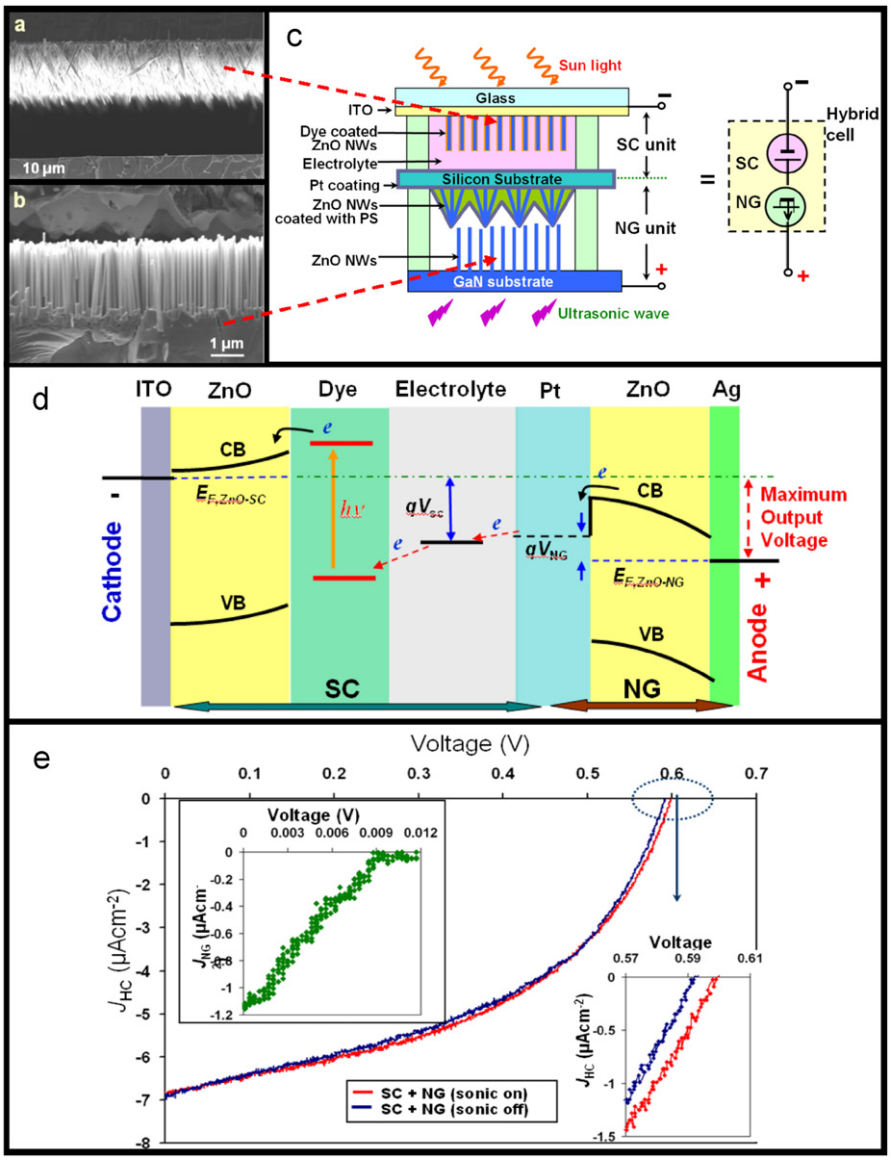

Figure 2 Design, structure, working principle, and performance of a hybrid cell (HC) composed of serially integrated solar cell (SC) and nanogenerator (NG) for raising the output voltage. (a) SEM image of ZnO nanowires (NWs) in the SC unit. (b) SEM image of ZnO NWs in the NG unit. (c) Schematic structure of a serially integrated HC, which is shined by sunlight from the top and excited by ultrasonic wave from the bottom. The ITO layer on the SC unit and GaN substrate are defined as the cathode and anode of the HC, respectively. The symbol to represent the HC is shown at the right-hand side. (d) Electron energy band diagram of the s-HC, showing that the maximum output voltage is a sum of those produced by SC and NG. The abbreviations are: conduction band (CB), valence band (VB), and Fermi level (E_F). (e) A comparison of *J*–*V* characteristics of a s-HC when illuminated by simulated sunlight with (red curve) and without (blue curve) turning on the ultrasonic wave excitation. Inset is an expanded output of the open circuit voltage U_{OC} points around the axial cross point, showing the increment of U_{OC} for ~9 mV after turning on ultrasonic waves. Both SC and NG were included in the measurement circuit.

deposited simultaneously with the NWs on the GaN substrate and the ITO glass served as the anode and the cathode of the HC, respectively.

The SC and NG units in the HC can work independently when either solar or mechanical energy source is available. The corresponding *J*-*V* (or *I*-*V*) curve of the NG shows that the $U_{OC\text{-}NG}$ was ~0.01 V and the J_{NG} was ~1.1 μA cm^{-2} (Fig. 2e). Since the output of the NG was much lower than that of the SC under full sun illumination, the SC output was purposely adjusted to a level comparable to that of the NG output by reducing the intensity of the illuminating light for the proof of the capability of simultaneously harvesting solar and mechanical energies. When the sunlight source was on and the ultrasonic wave (mechanical energy) was off, the HC exhibited a U_{OC} of 0.591 V and J_{SC} of 6.9 μA cm^{-2} (the blue curve in Fig. 2e). When both the mechanical and solar energy sources were turned on, the U_{OC} reached 0.60 V, while the J_{SC} remained at 6.9 μA cm^{-2} (red curve in Fig. 2e). The output voltage of the HC is differed by ~9 mV with or without the ultrasonic wave turned on, as shown by the expanded plot of U_{OC} in the inset of Fig. 2e, which shows the output voltage of the NG without sunlight.

Working principle of a hybrid cell

In semiconductor devices, an electron energy band diagram is usually used to depict the physics of the device. Xu et al. proposed the working principle [16] of the HC as shown in Fig. 2d. On the right-hand side of NG part, the maximum voltage output (V_{NG}) is determined by the difference between the Fermi level of the ZnO NWs (E_F, ZnO-NG) and that of the Platinum (Pt), which is suddenly lifted by electrons that have accumulated under the driving force of the piezoelectric potential from the NWs and the Ag on the bottom electrode. Under the mechanical deformation driven by external mechanical energy such as ultrasonic waves, a negative local piezoelectric potential is first created on the compressive side of an NW, which drives the accumulated charge carriers of the NW close to the Pt–ZnO junction to move and inject them into the Pt electrode because of the forward biased Schottky barrier effect. These electrons continue to be transported in the electrolyte through a redox reaction into the SC. The left-hand side of Fig. 2e shows the band structure of a ZnO based DSSC, where the maximum voltage output (V_{SC}) is dictated by the gap between the Fermi level of the ZnO (E_F, ZnO-SC) and the electrochemical potential of the electrolyte. When the light applied on the glass side of the HC excites the electrons to a high energy state of the dye molecules, they are subsequently transferred to the conduction band of the ZnO, and finally exported through the cathode at the Fermi level E_F, ZnO-SC. In the entire HC, electron energy is promoted twice by the NG and the SC, so the overall maximum output voltage is the sum of V_{SC} and V_{NG}. Later in this review, we will illustrate HC devices in which the overall performance is the sum of multi-energy harvesters.

Performance and reliability enhancement of a hybrid cell

The prototype of the HC that harvests both solar and mechanical energies uses both a DSSC and a piezoelectric NG. However, due to the encapsulation problem posed by the use of the liquid electrolyte in the conventional liquid-based DSSC, solvent leakage and evaporation become two major problems. The previous HC was actually a back-to-back physical integration of an NG and a DSSC on the same substrate, which may limit its performance. To solve these problems, early in 2011, Xu and Wang improved the prototype design of HC and developed a compact solid state hybrid cell [26] shown in Fig. 3a. The structure is still based on vertical ZnO nanowire arrays but with the introduction of solid electrolyte [27] and a metal coating (Fig. 3b). Here ITO served as the cathode while silver (Ag) paste in contact with GaN served as the anode (Fig. 3c). After the entire HC was connected to output wires, it was sealed and packaged by epoxy resin to prevent infiltration of any liquid except through window of the DSSC. In this HC device, the possibility of solvent leakage and evaporation from the DSSC is no longer an issue. The other advantage is that two energy harvesting parts are convolutedly designed in a single compact device, so it is truly a single device with the ability to simultaneously harvest both solar and mechanical energies.

The output current and voltage were measured using the same methods. The open circuit voltage ($U_{OC\text{-}SC}$) was 0.42 V, and the short circuit current density ($J_{SC\text{-}SC}$) was 0.25 mA cm^{-2} (Fig. 3d). The NG was characterized by introducing ultrasonic waves through the water media without sunlight illumination; the corresponding *J*-*V* curve shows that the $U_{OC\text{-}NG}$ was ~0.019 V and the I_{NG} was ~0.3 pA cm^{-2}.

To visually see the optimum power output from the *J*-*V* curve, the product of the current density and the voltage was calculated. The area of the rectangle represents the optimum output power density. The increase in the area of the rectangle (the blue curve to the red curve in Fig. 3d) shows that the HC enhances energy harvesting performance more than either one of the devices. When only simulated sunlight shines on the HC, the DSSC worked (Fig. 3d), and the optimum output power density (blue rectangle) was found to be 32.5 μW cm^{-2} at J_{SC} = 140 μA cm^{-2} and U_{OC} = 0.231 V. When both DSSC and NG were simultaneously operating in serial connection, the corresponding output power density was 34.5 μW cm^{-2} at J_{SC} = 141 μA cm^{-2} and U_{OC} = 0.243 V (red rectangle). After the ultrasonic wave was turned on, power density increased ($\triangle P_{HC}$) of 2 μW cm^{-2} which represented more than a 6% enhancement in optimum power output. Therefore, in addition to enhancing the open circuit voltage, the CHC successfully added up the total optimum power outputs from both the SC and the NG.

Although this study illustrates the successful demonstration of HC for simultaneously solar and mechanical energy harvesting, the HC devices sometimes cause crosstalk problems such as an increase in device series resistance and total volume resulting in degraded efficiency. Therefore, Choi et al. created a flexible HC [28] without any crosstalk and additional assembling process, so it differs from the previous integration process. The key advantages of this HC were that it requires no crosstalk, no volume increase, and no additional assembly process, and it produces synergetic effects on the performance of the elements. In this design, the characterization method is slightly different from the traditional illustration. The output signals from the solar energy harvester are direct

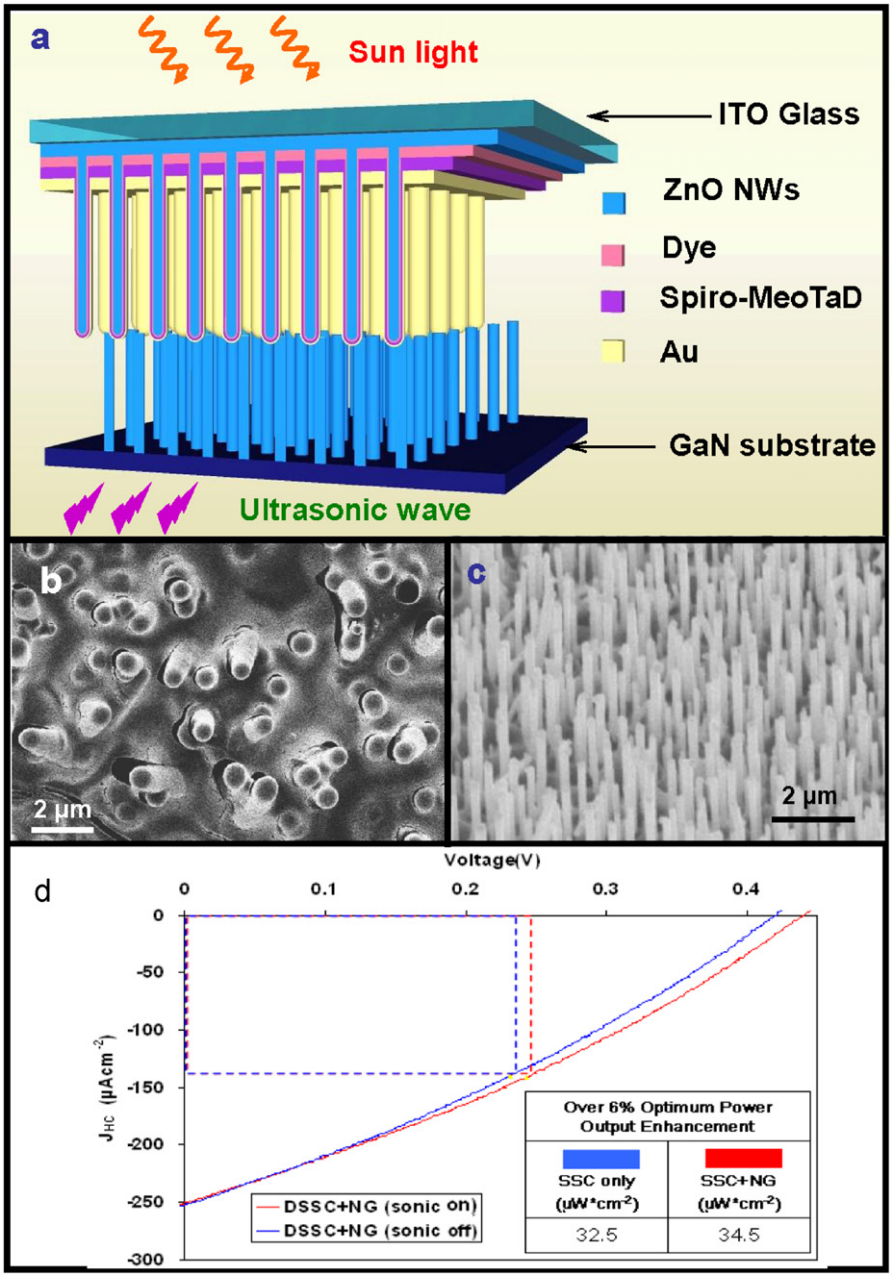

Figure 3 Design of the compact hybrid cell (HC) structure consisting of a SC and a NG. (a) Schematic illustration of a HC, which is illuminated by sunlight from the top and excited by ultrasonic waves from the bottom. The ITO layer on the DSSC part and GaN substrate are defined as the cathode and anode of the HC, respectively. (b) Top view SEM image of the DSSC. (c) SEM image of the as grown ZnO nanowire array using the high-temperature vapor deposition method for fabricating the NG. (d) A comparison in power output *J*–*V* characteristics of a HC. The rectangle area is the optimal power output for the HC.

current (DC), while the output signals from the mechanical energy harvester are originally an alternating current (AC) type in this design. By controlling the mechanical straining process, the AC signals could be tailored to a DC-like type. Based on such controllability of the output behavior, the performance, or output power of the HC was synergistically enhanced by the contribution of an NG, compared with that generated independently from the solar cell part under a normal indoor level of illumination (1 mW cm^{-2}).

The HC is based on the integration of an NG and an organic solar cell. To achieve a fully flexible power generating device, an indium tin oxide (ITO)-coated polyethersulfone (PES) substrate (Fig. 4a) was chosen as a cathode window in terms of a solar cell. A ZnO nanowire array was grown on the substrate, where was infiltrated with the P3HT:PCBM polymer blend, which created an electron channel conductor for transporting the electrons generated by the organic solar cell. The entire structure, which is flexible and packaged in a single platform, can be easily integrated with any flexible electronics. The power conversion efficiency (PCE) of about 1.5% on average from this HC was obtained with an open circuit voltage (U_{OC}) of 0.55 V and a short circuit current density (J_{SC}) of

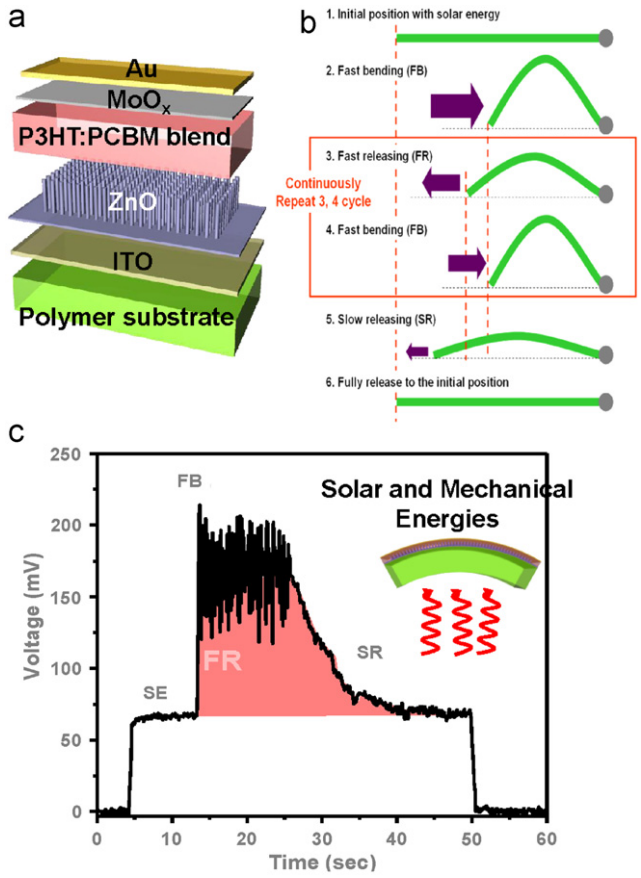

Figure 4 Design and performance of the serially connected flexible HC consisting of a SC and a NG. (a) Schematic illustration of detail structure of HC. To provide mechanical energy by bending, a transparent flexible polymer substrate is provided. (b) The detailed straining process. The green part is the HC device. (c) A comparison in output voltage measured by controlling straining processes under solar energy (SE) with fast bending (FB), fast release (FR), but not fully release, and slow releasing (SR) (figure courtesy of Choi et al. [28], with permission from Royal Chemical Society).

9.2 mA cm^{-2} in a standard AM 1.5 illumination condition (100 mW cm^{-2}) without any mechanical strain. In order to clearly present the AC output of HC as well as DC output, the voltage–time curve was characterized in Fig.4c. With a controlled mechanical straining process applied to the device, the overall output voltages from both solar and mechanical energies were synergistically enhanced. After fast bending of a hybrid device, the device was quickly released, although not fully, and then it was bent again to form the deformation cycle (see Fig. 4b for the details of the straining process). Since the device was not fully released, the negative piezoelectric pulse was much lower than the positive pulse, so a DC-like enhanced output voltage could be obtained as labeled the solar and mechanical energies curve in Fig. 4c. With such a "programmed" straining process, the total output voltage improved up to a factor of ~2 compared to that produced only by solar energy under room illumination. Considering that the reference solar power is fairly low, the hybrid device could be especially used in applications where there is a large amount of mechanical disturbance and the light intensity is rather low.

Although a flexible HC design that improves the voltage output has been developed, the enhancement of the current is also required. To achieve this goal, Xu et al. in recent work connected a ZnO nanowire-based DSSC to an NG with improved performance in parallel to form a HC (Fig. 5a). In this work, instead of generating direct current (DC), the NG generates alternating current (AC) output in synchronized with an external strain. The output current density of the HC contributed by the NG unit was about 0.3 μA/cm^2, and that of the SC unit was 0.95 μA/cm^2.

In this design, a double-side grown ZnO nanowire-based NG was chosen for the mechanical energy converter [29,30], and, based on the NG theory, generated voltage from the piezoelectric potential with the applied strain along the *c*-axis of the ZnO nanowire grown direction. Instead of using vertically aligned ZnO nanowires, ZnO nanowire textured films were grown on the top and bottom surfaces of a flexible polyester (PS) substrate (Dura-Lar, 220 μm in thickness) and scratched the top surfaces of these nanowires to bond the nanowires together tightly in a uniform film. Therefore, the entire ZnO nanostructure could be regarded as a textured thin film consisting of fully packed ZnO

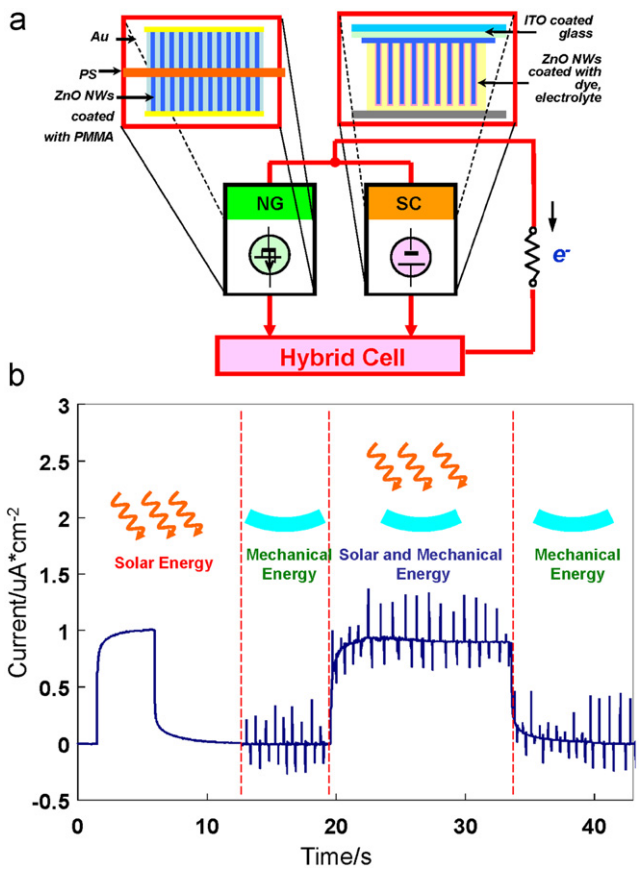

Figure 5 Design and performance of the parallel connected HC consisting of a SC and a NG. (a) SC is illuminated by sunlight from the top and NG is driven by linear motor. The ITO layer of SC and one side of Au electrode of NG are connected as cathode while Pt electrode of SC and the other side of Au electrode of NG are connected as anode. (b) A comparison in power output *J*–*t* characteristics of a parallel connected HC. HC is working independently and simultaneously.

nanowire arrays between two parallel ZnO nanowire films. According to the growth mechanism, the *c*-axes for these nanowires were their growth direction. Finally, after connecting two leads to the top and bottom electrodes, the entire device was fully packaged with polydimethylsiloxane (PDMS) to enhance the mechanical robustness and flexibility. Thus, each bending of the NG generated an electric pulse.

Considering the AC contribution of the HC, the multi-type energy harvesting function was characterized by recording the current–time curve in Fig. 5b. The operating of the HC devices is very similar to that of the flexible HC. The HC was tested with simulated light under simulating mechanical strain, which was generated by a linear motor that was accurately controlled by software. First, the simulated light (AM 1.5) was shined onto the HC, detecting the output of current density contributed from the solar unit of 0.95 $\mu A/cm^2$. After turning off the simulated light, periodic strain was applied to the HC at a frequency of 0.67 Hz instead of driving it by ultrasonic wave. Fig. 5b shows that the strain frequency was in consistent with the output current line. The compressed and tensile strains correspond to up and down peaks. During each cycle, the applied strain was maintained for 0.5 s; then it was withdrawn and NG was unstrained for 1 s before the next cycle. A maximum output of current density of 0.3 $\mu A/cm^2$ was received, as shown in the second column of Fig. 5b. Then the simulated light was turned on again and obtained a mesa enhancement of the current output. The AC current output varied from 0.65 $\mu A/cm^2$ to 1.25 $\mu A/cm^2$, confirming that both the solar and NG units contributed to the output. The fourth column shows that the mechanical contribution remains, even when the solar light was off.

Since the current output levels of the NG and the SC are comparable, small electronic devices can be driven by HCs with different types of energy [31,32]. With the HC device, the various sources of energy become more compatible and thus provide a reliable power source for small electronic devices.

Different types of hybrid cells

The nanostructure-based HCs developed for solar and mechanical energy harvesting have prompted considerable research effort to develop many different types of HCs. Researchers have been actively developing technologies capable of harvesting all available energy sources in our living environment in addition to solar and mechanical energies. Therefore, HCs have been developed by combining the harvesting of thermal and solar energies, sound and solar energies, and biochemical and mechanical energies. Others have also been developed for specific applications.

Hybrid cell for harvesting thermal and solar energies

During the energy conversion process in photovoltaic devices, the heat is usually the by-product of electricity that is lost in the past. To improve the energy conversion efficiency from the solar energy, in 2010, Guo et al. designed an HC to harvest the solar energy as well as the heat generated [33]. The HC consists of two parts: a DSSC and a thermoelectric cell (TC) comprising the upper and lower compartments. In the DSSC part, solar energy is firstly converted to electricity and heat. The heat is then transmitted to the TC used for thermoelectric conversion. The HC achieves higher efficiency than a single harvester and fully utilizes the energy from the sun.

The schematic of the HC is shown in Fig. 6a in which, the left part is the SC unit and the right part is the TC unit. When light is applied from the left side of the HC, the electron–hole pairs get separated and generate the photovoltaic potential. In addition to the photoelectric conversion, the DSSC also produces heat and transfers it to the TC which is made of semiconductor p–n junction. The temperature difference between the two sides of the TC changes the diffusion carrier density of the thermo-electric material that drives the incline of the Fermi level. The thermoelectric potential is thus generated. The overall output voltage output of the HC is determined by the sum of the DSSC and the TC.

In this design, the open circuit voltage U_{OC} of the HC increased from 723 mV (DSSC only) to 911 mV, which closely matched the sum of U_{OC} of the DSSC and the TC. The short

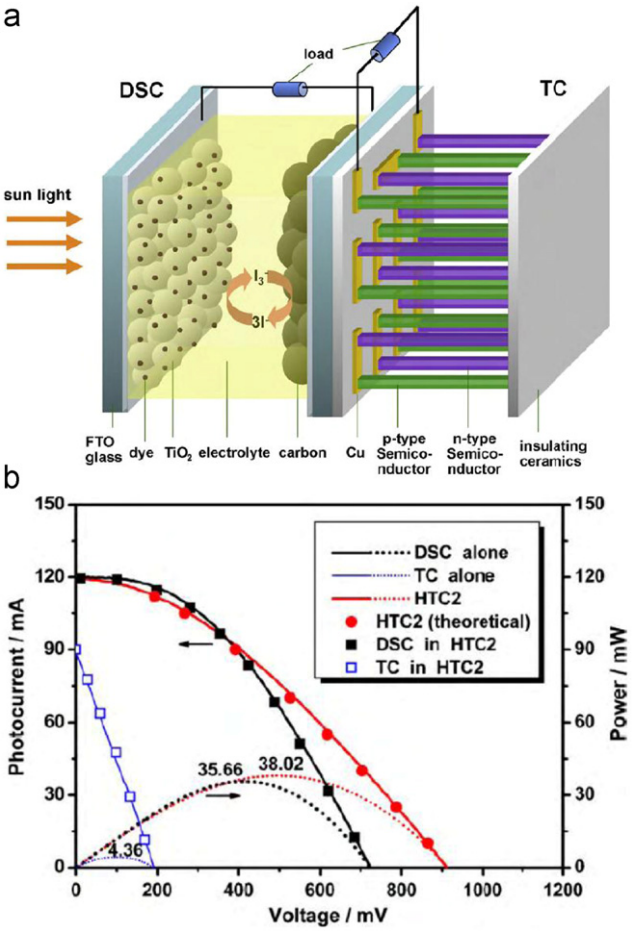

Figure 6 Design structure and performance of the HC for thermal and solar energy harvesting. (a) Schematic structure of HC consisting of a SC and a TC. (b) A *J*–*V* characteristic of the HC under AM 1.5 illumination. Circles are theoretical values of HTC; squares are the working status of SC (solid) and TC (hollow) while measuring HTC. (Figure Courtesy of Guo et al. [33] with permission from Journal of Power Sources.)

circuit current I_{SC} of the HC remained relatively unchanged, and a combined maximum output power of 38.02 mW was obtained (Fig. 6b). These experimental results were consistent with the theoretical results (circles in Fig. 6b) calculated from the photocurrent-voltage curves of the DSSC and the TC according to superposition theory. The results showed a good agreement with the photocurrent-voltage curves of the two parts under separated operations, which indicates that the performance of the DSSC and the TC remains unchanged after integration in the HC.

Hybrid cell for concurrently harvesting sound and solar energies

As a special mechanical energy source, the sound energy in the frequency range of 35–1000 Hz is commonly available in our daily life. In late 2010, Lee et al. designed an HC [34] specifically for harvesting sound and solar energies. The HC is based on a structure of a vertical NW array integrated NG (VING) with the infiltration of quantum dots (QDs) among the NWs, as shown in Fig. 7a. The vertically aligned NWs were responsible for harvesting sound energy, and the CdS (n-type)/CdTe (p-type) QDs were responsible for harvesting solar energy. Since the HC was composed of a pn-heterojunction of QDs and vertical NW arrays in contact with different metals such as ITO (top electrode) and Au (the bottom electrode), the two individual harvesters were connected in parallel.

In the case of SC unit, it generates direct current (DC) flow. Under sunlight illumination, the light passes through the transparent upper structures of the HC as well as the CdS layer underneath. Because of the photovoltaic potential generated at the interface of the CdTe/CdS pn-junction, electron–hole pairs are forcefully separated and accumulated in the CdS and CdTe QDs. A difference in the Fermi levels at the two electrodes drives the accumulated electrons in the CdS QDs to move toward the top ITO electrode, while the accumulated holes in the CdTe flow toward the bottom Au electrode. The DC output is thus created under constant solar illumination. According to the *I*–*V* curve under solar simulation (inset in Fig. 7b), the short-circuit current I_{SC} and the open-circuit voltage U_{OC} were found to be ~57 nA and ~6 mV, respectively.

However, in the case of VING unit, it generates alternating current (AC) output under an external acoustic waveform. As a result of application of a sound wave at a frequency of 50 Hz, a periodic force produced a short circuit current or an open-circuit voltage. The current output ranged from ~22 to 45 nA and the corresponding generated voltage was~1.5–6.0 mV. If we assume that the ZnO NW was under the compressive strain (Fig. 7b, red arrow and line), NWs have an elevated piezopotential near the bottom Au electrode. An elevated

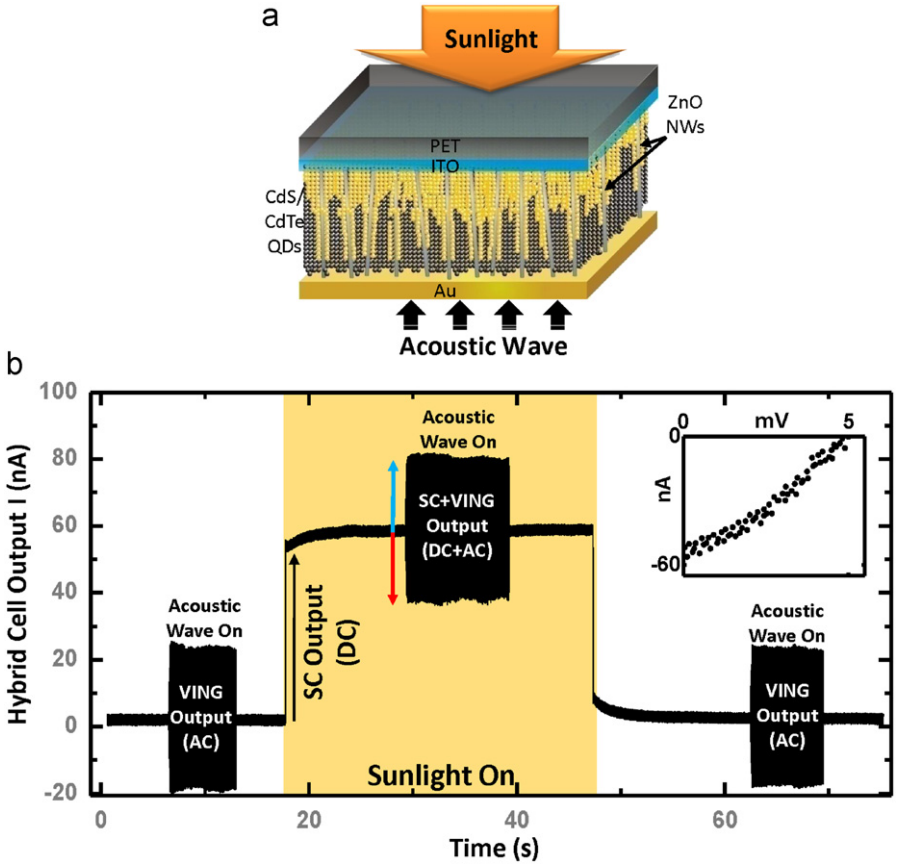

Figure 7 Design structure and performance of a HC for sound and solar energy harvesting. (a) Schematic diagram depicting a HC with two different incoming energy sources. Simulated sunlight illumination and acoustic vibration are delivered through the top PET/ITO layer and the bottom Au electrode, respectively. (b) Short-circuit current output signal of the HC. Acoustic wave was applied to the HC before/during/after solar illumination. Inset shows the *I*–*V* characteristic of a hybrid device under sunlight illumination.

inner potential of NWs drives the electron flow toward the external load from the bottom Au electrode, taking into account the presence of a Schottky barrier at the interface. When the NWs are under tensile strain (Fig. 7b, blue arrow and line), the polarity of the piezopotential is reversed, which drives the electron flow toward the external load from the top ITO electrode.

The concurrent-energy-harvesting performance was tested under the both acoustic wave environment and solar illumination. Acoustic waves (sound energy) were applied to the HC in the direction from the bottom Au electrode while a light source illuminated the embedded pn-heterojunction based on the CdS/CdTe QDs through the ITO coated PET layer. Fig. 7b shows the measured current signal versus time of the HC for easy illustration. When the acoustic wave was applied through the bottom Au electrode, the AC output with a peak-to-peak current of ~24 nA and a voltage of ~1 mV were scavenged by VING in the HC. From the middle section of Fig. 7b, the introduction of solar energy improved the current level by about 57 nA. In the third section, the current returned to the level it was after the light was turned off. Thus, this HC demonstrates the capability of harvesting solar and sound energies simultaneously.

Hybrid cell for biomechanical and biochemical energies

With the development of modern medical technology, powering implantable nanodevices for biosensing using energy harvesting technology has become a challenge. Because only mechanical, biochemical, and possibly electromagnetic energies can be harvested, while thermal and solar energies are not available for devices implanted inside the body because of the in vivo bio-environment. Specifically for this purpose, Hansen et al. in 2010 developed an HC device [35] for harvesting mechanical and biochemical energies [36] mainly for biomedical applications. Fig. 8a presents the design of this HC, which integrates nanowire-based NGs and enzymes-based biofuel cell (BFC).

In this hybrid design, Hansen et al. used piezoelectric poly(vinylidene fluoride) PVDF nanofibers (NF) as the working component for the mechanical energy harvester. The working principle of the PVDF NG is based on the piezoelectric properties of the PVDF NF. As the device being deformed under alternating compressive and tensile force, the NF drives a flow of electrons back and forth through the external circuit [37]. This charging and discharging process results in an AC output. Then the authors used an enzymatic BFC to convert the chemical energy of glucose and oxygen in the biofluid into electricity [38,39]. The electrodes were patterned onto Kapton film and coated with multiwall carbon nanotubes, and finally immobilized glucose oxidase (GO_x) and laccase to form the anode and cathode for BFC. When the device is in contact with a biofluid that contains glucose (such as blood), the corresponding chemical processes occurring at the two electrodes are as followed: glucose is electro-oxidized to gluconolactone at the anode, glucose (GO_x) → gluconolactone + $2H^+ + H_2O$, and dissolved O_2 is electro-reduced to water at the cathode, $1/2O_2 + 2H^+ + 2e^-$ (laccase) → H_2O. In the situation of human blood, a BFC can provide a U_{OC} of 50 mV and an I_{SC} of 11 nA [35].

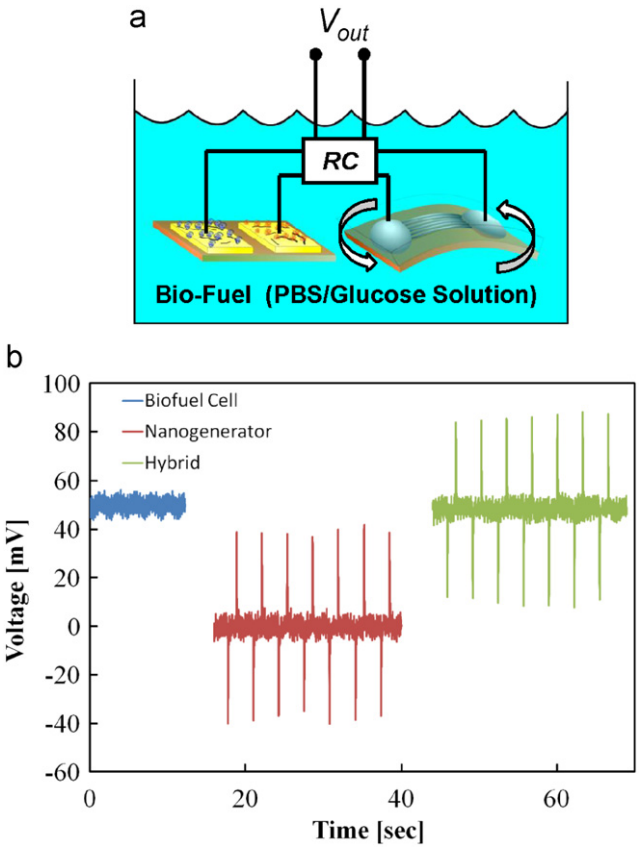

Figure 8 Design structure and performance of a HC for biochemical and biomechanical energy harvesting. (a) Schematic of HC device integration. Considering the inner resistance of the NG, the time required to charge the capacitor is much longer than the period at which the strain was applied to the NG, so that the output V is a sum of those from BFC and NG. (b) A comparison in open-loop V-t characteristic of the independent and combined operation of the BFC and NG.

However, one of the major hurdles of a glucose/O_2 BFC is the performance degradation over time resulting from the decay of the living enzymes. This HC made of BFC–NG shown in Fig. 8a, is able to not only harvest mechanical and biochemical energies, but also increase the power output and lifetime of the device. While the BFC part has the benefit of high power density, the NG part has the benefit of potentially much longer operating time, because its lifetime is limited only by the mechanical fatigue of the device. To integrate the AC voltage of the PVDF NG with the DC voltage of the BFC, a simple RC high-pass filter was used, which effectively blocks the DC voltage of the BFC in one direction while transmitting the AC voltage of the NG. By integrating the two devices, the peak voltage was nearly doubled from 50 to 95 mV (Fig. 8b). Furthermore, the PDMS packaging of the NG allows for operation inside biofluid and at in vivo environments.

The demonstrated HC device for biochemical and mechanical energy harvesting can work together to harvest multiple kinds of energy in bio-liquid. However, the two units of the previous HC were separately arranged on plastic substrate without integration, and the output was fairly low and the size was not compatible for practical applications.

In 2011, Pan et al. improved the design structure and device performance [40] with a flexible fiber based HC consisting of a fiber nanogenerator (FNG) and a fiber biofuel cell (FBFC). In this fiber based HC as shown in Fig. 9a, the FNG and FBFC are integrated on a single carbon fiber for the simultaneously or independently harvesting of mechanical and biochemical energies. In addition, the HC can also serve as a self-powered pressure sensor for detecting pressure variation in a bio-liquid, which will be described later. The design of the FNG is based on a core–shell structure in which the textured ZnO NW film (see the inset in Fig. 9a) is grown on the outer surface of the carbon fiber, which serves both the core electrode and the substrate for ZnO growth. While an FBFC for converting chemical energy from a bio-fluid is fabricated at the other end of the carbon fiber (Fig. 9a). Different from conventional biofuel cells, the FBFCs described here were integrated with the NG on a carbon fiber forming a HC. The elimination of the separator membrane and the mediator reduced the size of the FBFCs.

The performance of the HC was also characterized by measuring the short-circuit current I_{SC} and the open-circuit voltage U_{OC} versus time. The FBFC outputs were given as U_{FBFC} and I_{FBFC}, the AC FNG outputs as U_{FNG} and I_{FNG}, and the hybrid NG outputs as U_{HC} and I_{HC}. When the HC is immersed into a bio-liquid containing glucose, the FBFC generates a DC output. A typical FBFC output is: I_{FBFC} of ~100 nA and U_{FBFC} of ~100 mV. When a fixed pressure is periodically applied to the bio-liquid at an interval of 1.9 s for an extended period of 0.7 s, the FNG begins to generate an AC output. The general output of U_{FNG} is 3.0 V at an output current of I_{FNG} = 200 nA for an FNG consisting of ~1000 carbon fibers, and the corresponding current density is 0.06 mA cm^{-2}.

By integrating the AC FNG and DC FBFC, an HC with the output close to the sum of the FBFC and the FNG is obtained (Fig. 9b). The shape and frequency of the AC FNG output were the same before and after the hybridization process, with only the base line shifting from zero to the FBFC output. The peak value of the hybrid NG open-circuit voltage, U_{HC}, was $\pm$3.1 V when they were in series; the peak values of the short circuit current, I_{HC}, are 300 nA and −100 nA, when they were in parallel connection.

Hybrid cell for solar and biochemical energies

An integrated design of a DSSC and a BFC can make an HC on a common substrate that simultaneously harvests solar and chemical energies. Fig. 10a shows such a design. The top part is a BFC, and the bottom part is a DSSC. The solar light is incident from the bottom. Fig. 10b is the corresponding output

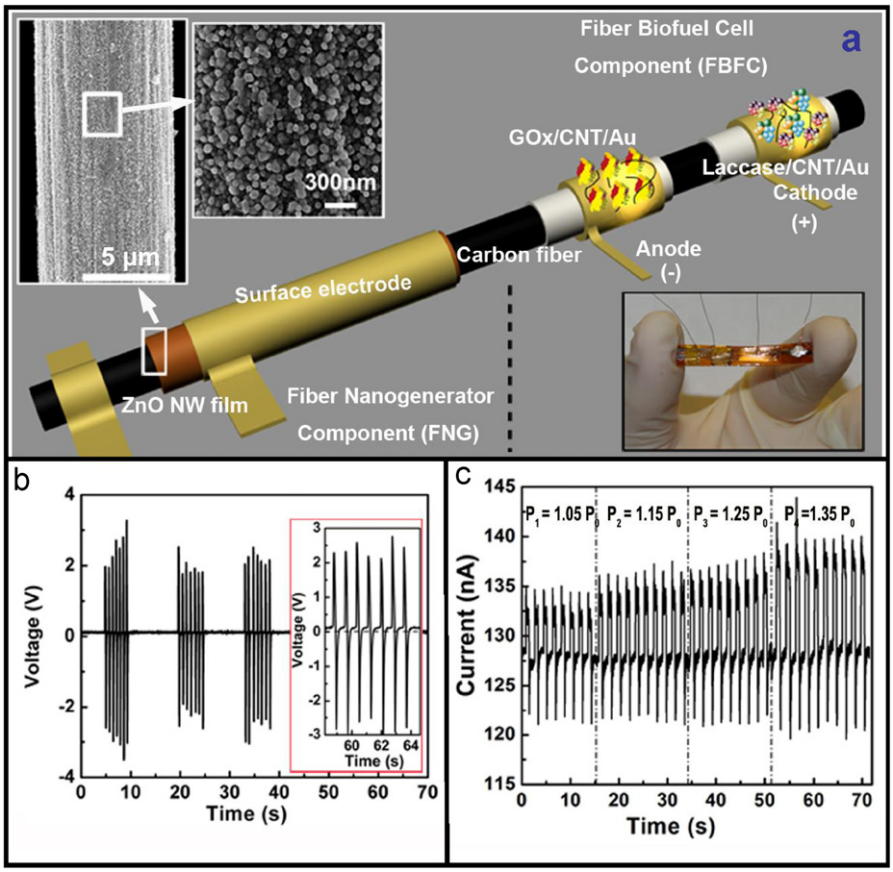

Figure 9 Design and pressure measurement of a single fiber-based HC for simultaneous harvesting of biochemical and mechanical energies from an external force or pressure applied to a liquid. (a) Schematic 3D representation of the HC. The insets in the upper left are SEM images of a textured ZnO NW film grown around a carbon fiber composed of densely packed ZnO NW to form a continuous textured film. A digital image of the device is shown at the lower corner. (b) A comparison in open-loop *V*-*t* characteristic of the HC when the FNG and the FBFC are connected in series. (c) Response of the HC system to periodically applied pressure.

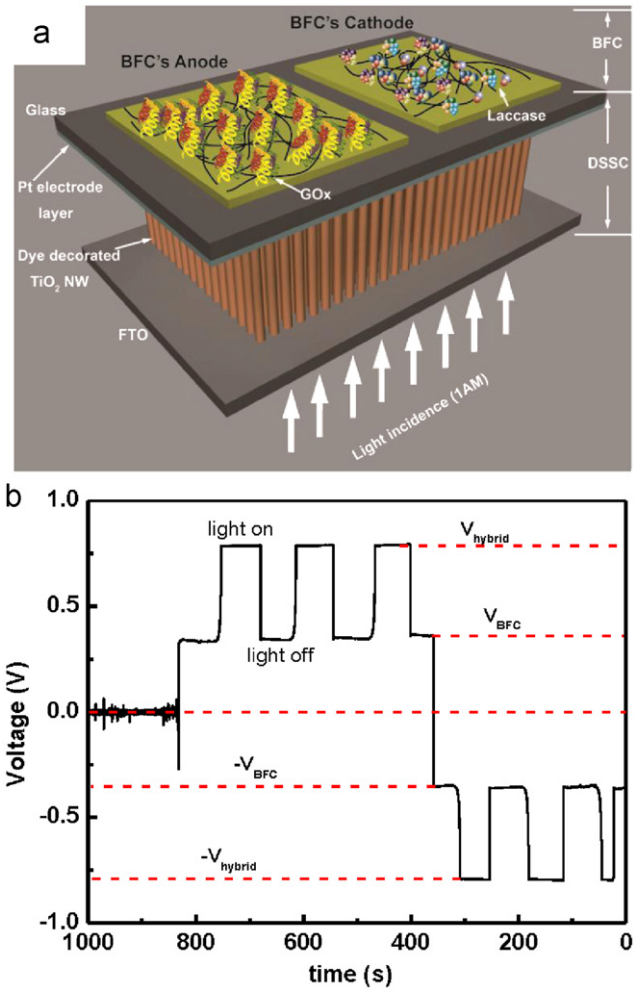

Figure 10 Integration of a solar cell and a biofuel cell as a HC. (a) Schematic diagram of the design. (b) Output voltage of an HC when the solar and BFC are in serial connection.

voltage of the HC, showing a linear superposition of the output voltage. When the two unites are in parallel, the output currents add up, but the output of the BFC is rather small. This experiment demonstrates the possibility of harvesting solar and chemical energies by an integrated unit.

Hybrid cell for driving small electronic devices

By utilizing these HCs, a number of applications such as powering a UV sensor, a pressure sensor, and a light emitting diode (LED) have been demonstrated as below. The success of HCs in this emerging field will lead to the use of such technology in numerous practical applications.

Self-powered UV sensor

The HC developed by Hansen et al. was also used to drive the operation of a ZnO nanowire-based UV light sensor [35]. The UV sensor and the HC are connected in a loop, as shown in Fig. 11a. The resistance of the ZnO nanowire in the HC was 7 MΩ without UV light shining on the top, and the corresponding peak voltage of the nanosensor declined

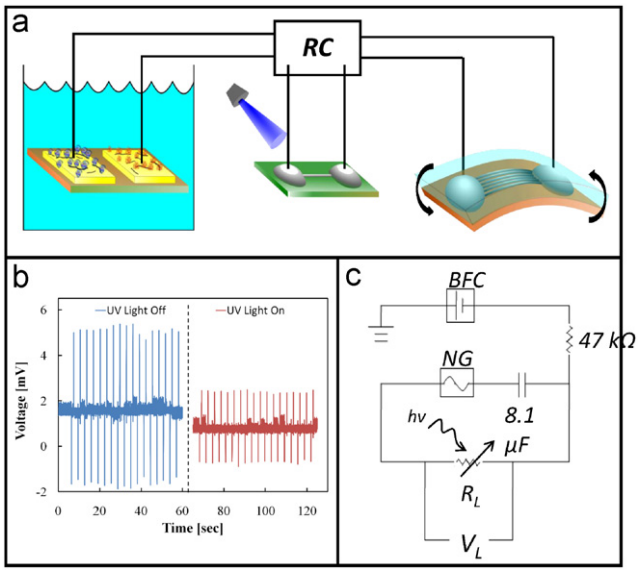

Figure 11 Integration of the HC device with a UV nanosensor to demonstrate a "self-powered" nanosystem. (a) Schematic illustration of the self-powered HC nanosystem. (b) A comparison in *V*-*t* characteristic across the ZnO NW UV light sensor when the UV light is off and on. For illustration purposes, only stabilized signals are displayed. (c) Circuit diagram used for integration of the HC device with a UV sensor.

5 mV, as depicted by the blue line in Fig. 11b. As a result of UV radiation, nanowire resistance declined to 800 kΩ and the peak voltage decreased to 2.5 mV. The output difference in voltage can be used to detect the UV light illumination. The work demonstrates the potential of a fully "self-powered" nanosystem. In addition, the HC was used to power a UV nanosensor, demonstrating the outstanding potential for a completely self-powered nanosystem for in vivo biomedical applications.

Self-powered pressure sensor

The fiber-based HC (Fig. 9a) developed by Pan et al. can also function as a self-powered nanosystem [40] for health care monitoring. The described HC has the potential to detect the pressure (or force) variation by changing the frequency, the interval time, and the holding time of the pressure application. The self-powered pressure sensor is created when the FNG and the FBFC are connected in series to form a loop similar to the one we discussed before. In this case, the FNG effectively works as a piezoelectric sensor, and the FBFC assumes the role of the power source that supplies the power to the FNG, forming a self-powered system for monitoring pressure variations in a bio-liquid.

From theoretical calculations, within the elastic linear mechanics regime, the output voltage of a single nanowire is proportional to the magnitude of its deformation. An increase in the pressure applied to the ZnO NW film leads to an increase in piezopotential, resulting in a higher current jump in the circuit. Current as a function of applied pressure is shown in Fig. 9c. When the applied pressure increased from ambient atmosphere P_0 to $1.05P_0$, $1.15P_0$, $1.25P_0$, and then $1.35P_0$, the response current increased

from 128 nA to 135 nA, that is, by roughly 7% (Fig. 9c). When pressure was applied, the response increased linearly, with a slope of ~19.2, following the relationship $\Delta I/I=0.192P/P_0-0.183$ (Fig. 9c). The sensitivity of the pressure measurement demonstrated was 1.35%. The fiber-based HC is capable of monitoring pressure in a liquid, such as blood pressure in a blood vessel by monitoring the current change in the circuit. This nanosystem is truly a self-powered hematomanometer, intended for monitoring tiny pressure variations in human blood vessel. It is well known that the human heart generates a periodic pulse pressure that is a complex time-dependent and nonlinear signal-reflecting the fluctuation of one's motion and health, resulting in fluctuations in blood pressure. A quantitative measurement of such a pressure signal could provide important information for health care and medical diagnostics in health care applications.

Powering an LED

As a power generation device, HCs could also be used to power up microelectronic device such as an LED. In recent work, Pan et al. demonstrated the powering of an LED successfully using an HC based on the BFC and NG. To fully use the electrical energy generated by the BFC and NG in the AC mode, a current rectification and energy storage system was implemented using a commercial full-wave bridge rectifier composed of four diodes (Fig. 12b), each with a threshold voltage of 0.3–0.4 V. Then the generated charge pulses were stored consecutively by connecting eight 22 μF capacitors in parallel, as shown in Fig. 12b, with the switches set at the "1" position. The entire charging process was recorded by monitoring the voltage/potential across a capacitor, presented in Fig. 12a, which shows a step increase in the stored energy corresponding to each cycle of the energy conversion process, as indicated by arrowheads in the inset of Fig. 12a. During the charging process, the voltage of the capacitor was saturated to ~0.2 V, which was lower than the peak output voltage of the HC, possibly resulting from the drop in the voltage, which was consumed at the rectifying diodes and/or the leakage of the capacitors, specifically when the capacitor voltage was high.

Then, by connecting eight charged capacitors in series by adjusting the switches to the "2" position (Fig. 12b), the total output voltage reached $V_{tot}=0.2\times 8=1.6$ V, which was high enough to drive an LED with a turn-on voltage of ~1.5 V, provided that the output power was sufficient at discharge. Using this voltage amplification technique, Pan et al. successfully powered a commercial LED by a fast discharge of the stored charges, as shown in Fig. 12c–e. After they were released to light up the LED, some of the charges remained in the capacitors.

Although the power generated by such a small HC cannot continuously drive an LED, an accumulation of charges generated over a period of time is capable of driving the LED for a fraction of a second. This function can be of practical use in devices that have standby and active modes, such as glucose sensors and blood pressure sensors for health monitoring, or even personal electronics such as Bluetooth transmitters (driving power ~5 mW; data transmission rate ~500 kbits s^{-1}; power consumption 10 nW per bit) that are

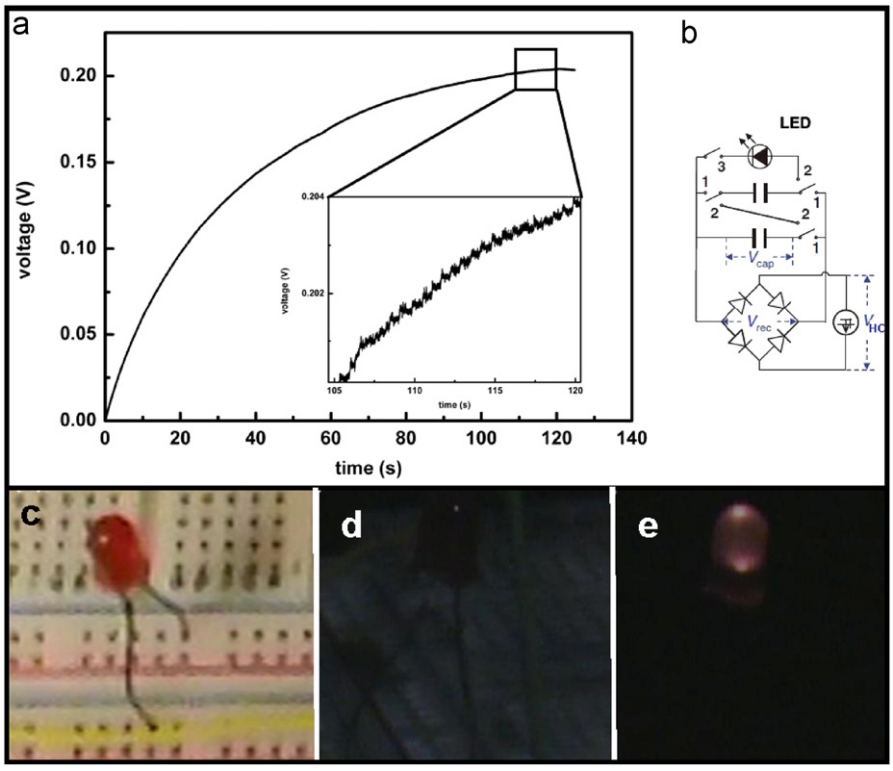

Figure 12 Using HC device to power an LED to demonstrate a practical application. (a) A *V*–*t* characteristic of charging process using the HC to collect the energy. (b) Circuit diagram used for the integration of the HC device with a bridge circuit to power an LED. (c) The regular LED in the circuit. (d) The unlighted LED. (e) The lighted LED by the HC.

only required to be in active mode for a very short period of time. The excess energy generated while the device is in standby mode is likely sufficient to drive the device when it is in active mode.

Conclusion

The search for sustainable power sources for driving nanosystems is an emerging field in today's energy research, and harvesting energy from multiple sources available in the environment to create self-powered nanosystems is now becoming a technological reality. This article has described a number of hybrid energy harvesting devices that can individually and simultaneously harvesting energy from ambient sources such as sunlight, thermo gradients, mechanical vibration, and electromagnetic waves. This review has mainly summarized the innovative approaches to using integrated structures/materials to create separated energy harvesting modules into a single package for multi-type energy harvesting. A comparison of enhancements in energy conversion efficiency and those in effective energy recovery processes have been illustrated. Potential applications have also been discussed to demonstrate that multiple types of energy in the environment can be utilized in an effective and complementary manner whenever and wherever one or all of them are available. As a new field in nanotechnology-related research, we anticipate to see the impact of HCs technology to nanosystem and even microsystems, which are intelligent, multifunctional, super-small, extremely sensitive, and energy efficient. Still in its incipient stages, the field is still wide open with many opportunities for study. More efforts on the part of both scientists as well as engineers will help advance HC technology. The development of this HC technology should also open up other novel research areas and challenging techniques.

Acknowledgments

Research was supported by DARPA, BES DOE, and NSF. We thank the contributions made by Dr. Xudong Wang, Dr. Youfan Hu, Wenxi Guo, Long Lin, and Ben Hansen to the materials reviewed here.

References

[1] R. Rapier 〈http://www.consumerenergyreport.com/2011/07/14/renewables-2011-global-status-report-released/〉.
[2] M.S. Dresselhaus, I.L. Thomas, Nature 414 (2001) 332–337.
[3] A. Hagfeldt, M. Gratzel, Accounts of Chemical Research 33 (2000) 269–277.
[4] M.K. Nazeeruddin, A. Kay, I. Rodicio, R. Humphrybaker, E. Muller, P. Liska, et al., Journal of the American Chemical Society 115 (1993) 6382–6390.
[5] B. Oregan, M. Gratzel, Nature 353 (1991) 737–740.
[6] W.U. Huynh, J.J. Dittmer, A.P. Alivisatos, Science 295 (2002) 2425–2427.
[7] Q.B. Pei, G. Yu, C. Zhang, Y. Yang, A.J. Heeger, Science 269 (1995) 1086–1088.
[8] G. Yu, J. Gao, J.C. Hummelen, F. Wudl, A.J. Heeger, Science 270 (1995) 1789–1791.
[9] B.Z. Tian, X.L. Zheng, T.J. Kempa, Y. Fang, N.F. Yu, G.H. Yu, et al., Nature 449 (2007) 885–U888.
[10] I. Gur, N.A. Fromer, M.L. Geier, A.P. Alivisatos, Science 310 (2005) 462–465.
[11] J.L. Mcnichols, W.S. Ginell, J.S. Cory, Science 203 (1979) 167–168.
[12] R.L. Liboff, Energy Source 3 (1978) 255–261.
[13] L. Eldada, Journal of Nanophotonics 5 (2011).
[14] F.J. DiSalvo, Science 285 (1999) 703–706.
[15] M.S. Dresselhaus, G. Chen, M.Y. Tang, R.G. Yang, H. Lee, D.Z. Wang, et al., Advanced Materials 19 (2007) 1043–1053.
[16] C. Xu, X.D. Wang, Z.L. Wang, Journal of the American Chemical Society 131 (2009) 5866–5872.
[17] Z.L. Wang, J.H. Song, Science 312 (2006) 242–246.
[18] Y. Cui, C.M. Lieber, Science 291 (2001) 851–853.
[19] Z.W. Pan, Z.R. Dai, Z.L. Wang, Science 291 (2001) 1947–1949.
[20] Z.L. Wang, Scientific American 298 (2008) 82–87.
[21] M. Law, L.E. Greene, J.C. Johnson, R. Saykally, P.D. Yang, Nature Materials 4 (2005) 455–459.
[22] M. Gratzel, Nature 414 (2001) 338–344.
[23] X.D. Wang, J.H. Song, J. Liu, Z.L. Wang, Science 316 (2007) 102–105.
[24] X.D. Wang, J.H. Song, C.J. Summers, J.H. Ryou, P. Li, R.D. Dupuis, et al., Journal of Physical Chemistry B 110 (2006) 7720–7724.
[25] S. Xu, Y. Qin, C. Xu, Y.G. Wei, R.S. Yang, Z.L. Wang, Nature Nanotechnology 5 (2010) 366–373.
[26] C. Xu, Z.L. Wang, Advanced Materials 23 (2011) 873.
[27] U. Bach, D. Lupo, P. Comte, J.E. Moser, F. Weissortel, J. Salbeck, et al., Nature 395 (1998) 583–585.
[28] D. Choi, K.Y. Lee, M.J. Jin, S.G. Ihn, S.Y. Yun, X. Bulliard, et al., Energy and Environmental Science 4 (2011) 4607–4613.
[29] Y.F. Hu, Y. Zhang, C. Xu, G.A. Zhu, Z.L. Wang, Nano Letters 10 (2010) 5025–5031.
[30] L. Lin, C.H. Lai, Y.F. Hu, Y. Zhang, X. Wang, C. Xu, et al., Nanotechnology 22 (2011).
[31] Y.F. Hu, Y. Zhang, C. Xu, L. Lin, R.L. Snyder, Z.L. Wang, Nano Letters 11 (2011) 2572–2577.
[32] Y.F. Hu, C. Xu, Y. Zhang, L. Lin, R.L. Snyder, Z.L. Wang, Advanced Materials 23 (2011) 4068.
[33] X.Z. Guo, Y.D. Zhang, D. Qin, Y.H. Luo, D.M. Li, Y.T. Pang, et al., Journal of Power Sources 195 (2010) 7684–7690.
[34] M. Lee, R. Yang, C. Li, Z.L. Wang, Journal of Physical Chemistry Letters 1 (2010) 2929–2935.
[35] B.J. Hansen, Y. Liu, R.S. Yang, Z.L. Wang, ACS Nano 4 (2010) 3647–3652.
[36] R. Yang, Y. Qin, C. Li, G. Zhu, Z.L. Wang, Nano Letters 9 (2009) 1201–1205.
[37] R.S. Yang, Y. Qin, L.M. Dai, Z.L. Wang, Nature Nanotechnology 4 (2009) 34–39.
[38] A. Heller, Physical Chemistry Chemical Physics 6 (2004) 209–216.
[39] N. Mano, F. Mao, A. Heller, Journal of the American Chemical Society 125 (2003) 6588–6594.
[40] C. Pan, Z. Li, W. Guo, J. Zhu, Z.L. Wang, Angewandte Chemie International Edition 50 (2011) 11192–11196.

Chen Xu received his B.S. (2007) in Electrical Engineering and was entitled as a "Wang Dao Scholar" from Fudan University. He is currently a Ph.D. candidate in the School of Materials Science and Engineering at Georgia Institute of Technology. He is working as a graduate research assistant in Prof. Z.L. Wang's group. His research mainly focuses on the integration of nanowire-based devices including piezoelectric-nanowire-based devices and nano-enabled photovoltaic devices and developing novel processes for the integration of top-down and

bottom-up approaches in nanoscale devices. Contact him at the School of Materials Science and Eng., 771 Ferst Dr. NW, Georgia Inst. of Technology, Atlanta, GA 30332; cxu9@mail.gatech.edu.

Caofeng Pan received his B.S. degree (2005) and his Ph.D. in (2010) in Materials Science and Engineering from Tsinghua University, China. He is currently a research scientist in the group of Professor Zhong Lin Wang at the Georgia Institute of Technology. His main research interests focus on the fields of nano-power source (such as nanofuel cell, nano-biofuel cell, and nanogenerator), hybrid nanogenerators, piezotronics, and piezo-phototronics for fabricating new electronic and optoelectronic devices.

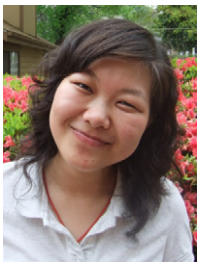

Ying Liu received her B.S. in physics from the Yuanpei Program (the first multidiscipline and liberal art undergrad program in China) at Peking University in 2009 and is currently a Ph.D. candidate in Prof. Z.L. Wang's group in School of Materials Science and Engineering at the Georgia Institute of Technology. Her research is mainly motivated by the fundamental physics in new phenomena with potential benefit for mankind, including applications in energy and electronics. During her graduate study, she has been working on nano-piezotronics, including fabrication of hybrid nanogenerators, and theory and calculation of piezopotential and piezotronics in various nanomaterials. Her recent research is focusing on theory and experiments of piezo-phototronics, including piezo-charges tuned photodetection, piezo-charge enhanced light emitting diodes, and self-powered phototronic systems.

Zhong Lin (ZL) Wang received his Ph.D. from Arizona State University in physics. He now is the Hightower Chair in Materials Science and Engineering, Regents' Professor, Engineering Distinguished Professor and Director, Center for Nanostructure Characterization, at Georgia Tech. Dr. Wang has made original and innovative contributions to the synthesis, discovery, characterization, and understanding of fundamental physical properties of oxide nanobelts and nanowires, as well as applications of nanowires in energy sciences, electronics, optoelectronics, and biological science. His discovery and breakthroughs in developing nanogenerators establish the principle and technological road map for harvesting mechanical energy from environment and biological systems for powering a personal electronics. His research on self-powered nanosystems has inspired the worldwide effort in academia and industry for studying energy for micro-nano-systems, which is now a distinct disciplinary in energy research and future sensor networks. He coined and pioneered the field of piezotronics and piezo-phototronics by introducing piezoelectric potential gated charge transport process in fabricating new electronic and optoelectronic devices. Details can be found at http://www.nanoscience.gatech.edu.